The Northern Walker Lane: How Complex is it? Quantifying Geodetic and Geologic Strain in the Western Basin and Range Using Enhanced Block Modeling Algorithms

William C. Hammond, Corné Kreemer, Geoffrey Blewitt

Nevada Geodetic Laboratory

Nevada Bureau of Mines and Geology and Seismological Laboratory

University of Nevada, Reno

whammond@unr.edu

Introduction

Crustal deformation in the northern Walker Lane accommodates roughly 25% of the Pacific/North America relative motion. In contrast to other parts of this plate boundary system, the regional patterns of faulting are complex, and are not completely described. In particular, the role and importance of crustal block rotations, fault system step-overs, and off-fault deformation are not well understood. Furthermore, given the present state of knowledge there is a large discrepancy between geologically and geodetically observed deformation rates, which suggests a fundamental gap in knowledge and/or understanding of this important part of the plate boundary.

Geodetic velocities along with fault trace geometries and seismicity patterns are often used to create and constrain analytical block models of crustal deformation. However, drawing the block boundaries sometimes requires a certain degree of assumptions and subjective judgment as to how individual fault segments are connected to form through-going fault systems and prevent kinematic inconsistencies. Furthermore, other assumptions are implicitly applied such as that all the deformation is accommodated on well-defined faults, implying that strain accommodated on other types of structures such as folds, dike intrusions, and distributed strain are not important for accommodating long-term motions. In many localities where fault systems are relatively simple, this approach may work well. However in the northern Walker Lane the complexity of the system and the gaps in our knowledge may suggest that we can improve our understanding if we 1) take an integrative approach that incorporates geologic and geodetic data, 2) allow for structures that we have not imagined, and 3) allow for the possibility that incongruous geodetic and geologic data may be reconciled by fault slip rates that vary over time. Evaluating the characteristic size of blocks that are needed to explain the data is an important step in determining the limiting size scale to which intracontinental deformation is block-like or continuum-like.

Here we go over our strategy for implementing innovations in block modeling, including an iterative non-linear algorithm that refines estimates of the deformation pattern and selects block boundaries that best fit the geodetic and geologic data. As constraints we use northern Walker Lane/western Basin and Range GPS velocities from 1) PBO sites, 2) BARGEN continuous sites , 3) our own MAGNET semi-continuous network which has a roughly 20 km station spacing, 4) USGS campaign GPS data.

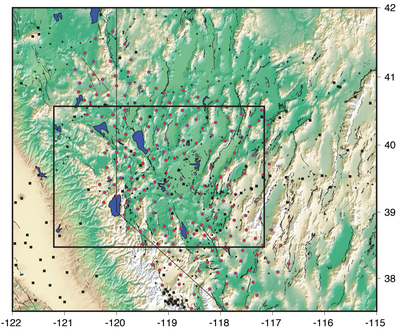

Left) The Northern Walker Lane of California and Nevada is the region east of the Sierra Nevada and west of the central Great Basin. Topography is disrupted and follows a different grain, compared to the more classic Basin and Range topography to the east. The black outline indicates the region that we model. Approximately 10 mm/yr of extension and dextral shear are accommodated across this box as the Sierra Nevada translates northwest with respect to the central Great Basin.

GPS sites whose data we use to constrain deformation are indicated with:
red dots: Univ. of Nevada MAGNET semi-continuous
black squares: PBO, BARD and BARGEN continuous sites
black plus signs: USGS campaign sites

Faults are shown with black lines. Blue patches are major lakes (e.g. Tahoe, Pyramid, Walker, Honey, Lahontan, etc.)

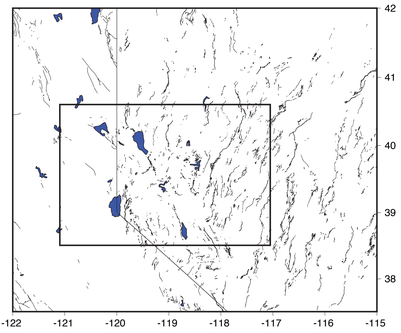

Slip rates based on geologic studies and summed across the northern Walker Lane fall far short of the geodetically estimated 10 mm/yr (by a factor of 2-3). To make comparisons between geodetically and geologically estimated fault slip rates we model the slip on faults using blocks whose motion is constrained by GPS measurments.

Left) Faulting in the northern Walker Lane and western Basin and Range is extensive and complex. The Basin and Range faults strike north-northeast and follow a fairly consistent grain that is consistent with extension in a roughly west-northwest direction. The Walker Lane faults have less consistent strikes, but can be loosely classified into three groups 1) north striking normal faults that accommodate ~east-west extension, 2) northwest striking dextral slip faults, and 3) northeast striking sinistral faults [e.g. *Wesnousky*, 2005]. This pattern of strain accommodation is broadly consistent with the GPS results which show the Walker Lane to be a zone of focused transtension accommodating ~10 mm/yr of relative motion.

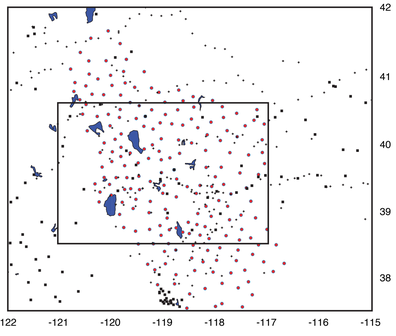

Left) GPS data coverage in the area has improved dramatically in the past several years. The combined networks of PBO, the University of Nevada, BARGEN, and USGS now provide coverage that is in places better than 20 km spacing.

The MAGNET network alone consists of ~250 sites that are measured with 55 Trimble GPS receivers, with observation schedules that vary from full time observation to episodic (1-3 year period). Inside the box at left the sites are most commonly observed about 1/3 of the time, which yields reliable velocities nearly as precise as continuous sites in ~2.5 years. The coverage is most dense and the network is most mature (i.e. sites have been observed for the longest time) inside the box.

GPS sites whose data we use to constrain deformation are indicated with:
red dots: Univ. of Nevada MAGNET semi-continuous
black squares: PBO, BARD and BARGEN continuous sites
black plus signs: USGS campaign sites

Smooth

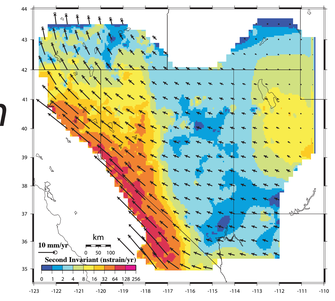

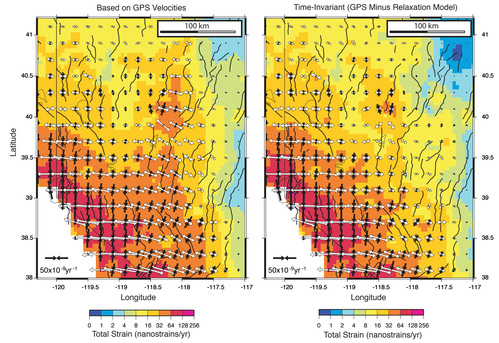

DISCRETE BLOCKS VS. CONTINUUM

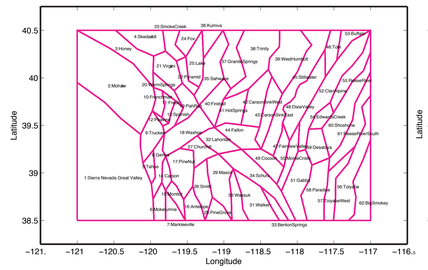

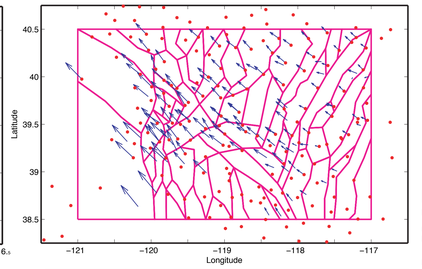

Lots of Blocks vs. Few Blocks

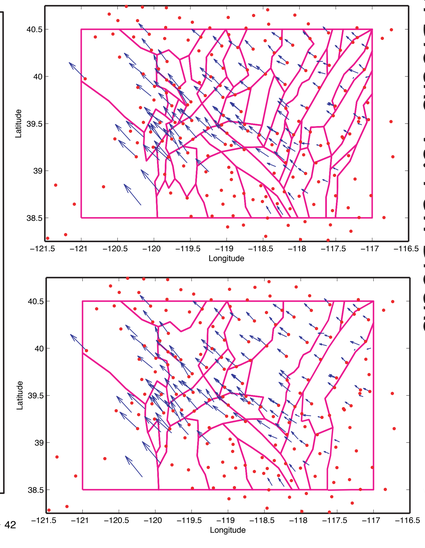

Continuum vs. microplate...
...models currently compete for the best explanation of intracontinental deformation patterns [e.g *England and McKenzie*, 1982; *Thatcher* 1995, 2003]. The northern Walker Lane, however, may possess qualitites of both. As the quality and quantity of GPS data on crustal deformation in the Walker Lane improves, the fidelity of our modeling of the patterns of deformation needs to keep pace.

We ask the question: Is it possible to infer slip rates on faults at the scale of individual crustal blocks (individual basins and ranges) given that we have several high quality continuous or semi-continuous GPS sites on each block? And if not, what is the minimum size of a block that can be identified as stable? In answering this question we place a spatial limit on the blockyness of continental deformation.

Iterative Block Boundary Deselection
We begin with a block model that is purposefully more detailed that can likely be constrained from the existing set of GPS measurements. The model above has 62 blocks with boundaries that adhere to the major range-front faults and other faults that have been identified as active in the part of the northern Walker Lane where data collection has made the most progress. We solve for block motions and slip rates according to the strategy detailed at the far right of this poster. We then progressively remove block boundaries that do not have an impact on the misfit to the data, until we arrive at a model that has the minimum complexity that can be justified by our data.

Blocky

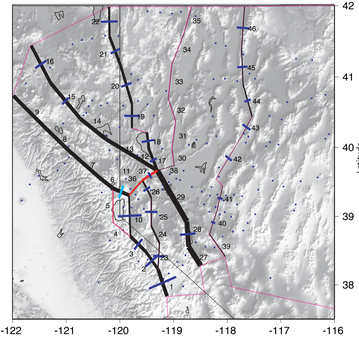

Above) A block model of the northern Walker Lane constrained primarily by campaign data and a few continuous sites from the BARGEN network (from Hammond and Thacther, 2007 in press). This model has 9 blocks.

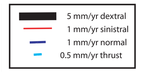

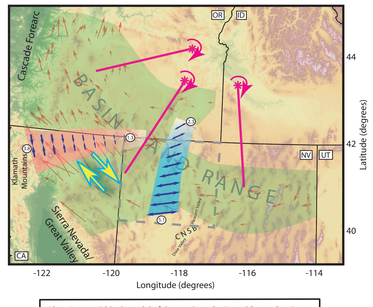

Above) a quasi-block model of the northern Basin and Range Province constrained by GPS velocities (red vectors). Here the light green patches are domians that rotate rigidly around nearby poles (magenta stars). The exception is the northeast CA domain which undergoes shear strain in addition to block rotation. The blue and red zones denote areas of east-west extension and north-south contraction respectively. Numbers in white circles show relative motion in mm/yr.

Continuum Models

Continuum models are valuable because they allow us to visualize and interpret the first-order characteristics of the deformation field. The Basin and Range continuum strain rate model (far left) of *Kreemer et al.*, (2007) shows the concentration of strains at the province boundaries and the general increase of intensity in strain close to the Sierra Nevada microplate. Continuum models also allow for the interpretation of the style of deformation (see tensor strain rate axes left and middle left), and compare it to fault strike. This allows for a comparison between the patterns of strain accumulation vs. strain release.

Also shown is the effect of a correction for post-seismic relaxation that perturbs the modern geodetic velocity field (immediate left). This effect needs to be taken into account when comparing geodetic data to geologic data. It is attributable to viscoelastic relaxation following the 20th century earthquakes of the central Nevada Seismic Belt [Gourmelen and Amelung, 2005; Hammond et al., 2007].

GPS constraints

Currently we have 130 GPS velocity vectors inside our study area that are sufficiently accurate (uncertainty <1 mm/yr) to constrain crustal deformation (blue vectors at left). These are from an integrated solution of all PBO, BARGEN, MAGNET, and campaign data avilable to us.

Because of PBO and our efforts in developing MAGNET, the next couple of years will see a further increase in the number of GPS velocities in our study area. The red dots (left) indicate sites where GPS data has been collected, but is so far insufficient to constrain a velocity reliably. In the next couple of years, the most detailed block model (having the greatest number of blocks, above left) will have velocities constraining every every block.

Results to Date

So far we have developed and coded in matlab the core block modeling algorithm (see box upper right) that infers block motions and slip rates (see example results below far left) and strains within the blocks. In preparation for development of the non-linear iterative block boundary removal, we have developed an algorithm that removes block boundaries given a boundary segment, providing a simpler model.

The example block models (left) indicate schematically how iterative block boundary removal will reduce model complexity until the data are violated.

Currently our most challenging problem is regularizing the inversion when the number of blocks is large compared the spatial density of GPS velocities. This problem is simiar to tomographic inverstions where the number of model parameters is greater than the number of data. As in tomography, stochastic damping and smoothing will be applied to find the simplest model that can explain the data.

Block Models

Block models are valuable because they allow us to estimate slip rates on specific fault systems or evaluate the rigidity/non-rigidity of specific tectonic domains. Slip rates are important to quantify because calcuations of seismic hazard are sometimes based on average activity of specific faults. Thus estimating slip rates with GPS allows geodesy to complement data on historic and paleoseismicity.

This exercise also allows for comparison between the patterns of strain accumulation (that is measured geodetically) to the pattens of strain release (that is measured by seismologists and by paleoseismologists).

Block Modeling Strateg

We assume that the surface motion can be approximated as piecewise continuous block rotations on a sphere, and that at the boundaries of the blocks are in contact, locked at the surface but slipping continuously at depth (e.g. *Savage and Burford*, 1973). Since our strategy for extending the concept to many blocks bounded by finite fault segments is similar to those of other recently introduced block modeling schemes (e.g. *Bennett et al.*, 1996; *Prawirodirdjo et al.*, 1997; *Souter*, 1998; *McClusky et al.*, 2001; *Murray and Segall*, 2001; *McCaffrey*, 2002; 2005; *Meade and Hagar*, 2005) we express our formulation briefly. We further assume that the GPS velocities represent the interseismic velocity field, i.e. they have been measured between large earthquakes and the effects of non–secular processes are either non–existent or have been estimated and removed. Thus, the long–term velocity (averaged over many seismic cycles) is equal to the sum of the interseismic and coseismic velocity

$$\vec{v}_{LT} = \vec{v}_{IM} + \vec{v}_{CO},$$

or equivalently

$$\vec{v}_{IM} = \vec{v}_{LT} - \vec{v}_{CO}.$$

This implements the "back–slip" approach introduced by *Savage* [1983]. In this context "coseismic velocity" is defined as the rate of movement of a point near the fault associated with coseismic offsets averaged over many seismic cycles.

For GPS velocity vector i with position $\vec{r}_i$ on block j

$$\vec{v}_{GPS,j} = \vec{\omega}_j \times \vec{r}_i - (a_j \vec{G}_{SS,k} + b_j \vec{G}_{N,k})$$

where $\vec{\omega}_j$ is an unknown block rotation vector. The slip rates a_k and b_k are unknowns that scale the Greens functions G_{SS} and G_N representing the pattern of strike slip and normal slip respectively for each fault segment k. These Green's functions are calculated for each fault segment using the functions of *Okada*, [1985,1992], since the dip, length, width and depth of the fault are predefined and unit slip is assumed to be sinistral for G_{SS} and up–dip for G_N. Since GPS sites can be affected by elastic strain accumulation on more than one fault segment, especially in complex zones with densely spaced faults, we modify to include the effects of multiple nearby fault segments

$$\vec{v}_{GPS,j} = \vec{\omega}_j \times \vec{r}_i - \sum_{k=1}^{L} (a_k \vec{G}_{SS,k} + b_k \vec{G}_{N,k})$$

where L is the number of nearest fault segments included.

Since our data comprise only horizontal components of velocity, we project the model into the horizontal plane before writing out the matrix equation

$$\vec{v}_{N,j} = \left[\vec{\omega}_j \times \vec{r}_i - \sum_{k=1}^{L} (a_k \vec{G}_{SS,k} + b_k \vec{G}_{N,k})\right] \bullet \vec{e}_N$$
$$\vec{v}_{E,j} = \left[\vec{\omega}_j \times \vec{r}_i - \sum_{k=1}^{L} (a_k \vec{G}_{SS,k} + b_k \vec{G}_{N,k})\right] \bullet \vec{e}_E$$

where $\vec{e}_N$, and $\vec{e}_E$, are the unit basis vectors at site i in the north and east directions respectively.

We wish to explicitly account for strain that can occur in each block that is not taken up on the boundary of the blocks. We do this in case the blocks are large and some faults exist inside the block, or if some deformation is taken up by processes other than faulting (e.g. folding, distributed postseismic deformation, etc.). We add terms to the equation that allow us to explain some of the velocities with secular strains

$$\vec{v}_{N,j} = \left[\vec{\omega}_j \times \vec{r}_i - \sum_{k=1}^{L} (a_k \vec{G}_{SS,k} + b_k \vec{G}_{N,k})\right] \bullet \vec{e}_N - \varepsilon_{\phi\phi} r_0 \sin\theta_0 \Delta\phi - \varepsilon_{\theta\theta} r_0 \Delta\theta$$
$$\vec{v}_{E,j} = \left[\vec{\omega}_j \times \vec{r}_i - \sum_{k=1}^{L} (a_k \vec{G}_{SS,k} + b_k \vec{G}_{N,k})\right] \bullet \vec{e}_E + \varepsilon_{\phi\theta} r_0 \sin\theta_0 \Delta\phi + \varepsilon_{\phi\theta} r_0 \Delta\theta$$

where $\varepsilon_{\phi\phi}$, $\varepsilon_{\phi\theta}$, $\varepsilon_{\theta\theta}$ are the strains in co–latitude θ, longitude ϕ space following *Savage et al.*, 2001, r_0 is the radius of the Earth, θ_0 is the co–latitude of the site, $\Delta\phi$ and $\Delta\theta$ are the angular distance from the center of the block to the site.

However, the slip rates on faults (a_k and b_k) are completely determined by the relative motion of the blocks and the predefined block geometries and fault dips. Thus, effectively the only parameters that need to be free are the block rotations (ω_j). To enforce this we write an additional constraint that the relative motion of the blocks should be related to the slip rate at the fault (ignoring strain inside the block)

$$\vec{\omega}_{j_1} \times \vec{p}_k - \vec{\omega}_{j_2} \times \vec{p}_k = a_k \delta\vec{G}_{SS,k} + b_k \delta\vec{G}_{N,k}$$

where $\delta\vec{G}_{SS,k}$ and $\delta\vec{G}_{N,k}$ are respectively the full strike slip and dip–slip motion vector slip rates in the global reference frame across fault k defined as

$$\delta\vec{G}_{SS,k} = \vec{G}_{sk}(\vec{p}_k + \vec{e}) - \vec{G}_{sk}(\vec{p}_k - \vec{e})$$
$$\delta\vec{G}_{N,k} = \vec{G}_{nk}(\vec{p}_k + \vec{e}) - \vec{G}_{nk}(\vec{p}_k - \vec{e})$$

where $\vec{e}$ is a small vector that points in a horizontal direction normal to the fault segment, and $\vec{p}_k$ is the mid–point of fault segment k. This constraint is equivalent to assuming that the horizontal long–term rate of relative motion across block boundaries is equal to the horizontal projection of the slip rate on the fault. The distinction is important because it is the basis for forcing the slip rate on the fault to be determined by all data on the block, not just data near the fault.

If we take the secular strain inside the block into account, apply the dot products to resolve the relative motions onto horizontal coordinates and apply the identity

$$\vec{u} \bullet (\vec{v} \times \vec{w}) = -\vec{v} \bullet (\vec{u} \times \vec{w})$$

we obtain

$$v_{N,j} = -\vec{\omega}_j \bullet (\vec{G}_{SS,j} \times \vec{r}_i) - \left[\sum_{k=1}^{L} (a_k \vec{G}_{SS,k} + b_k \vec{G}_{N,k})\right] \bullet \vec{e}_{N,j} - \varepsilon_{\phi\phi} r_0 \sin\theta_0 \Delta\phi - \varepsilon_{\theta\theta} r_0 \Delta\theta$$
$$v_{E,j} = -\vec{\omega}_j \bullet (\vec{G}_{E,j} \times \vec{r}_i) - \left[\sum_{k=1}^{L} (a_k \vec{G}_{SS,k} + b_k \vec{G}_{N,k})\right] \bullet \vec{e}_{E,j} + \varepsilon_{\phi\theta} r_0 \sin\theta_0 \Delta\phi + \varepsilon_{\phi\theta} r_0 \Delta\theta$$

$$\vec{\omega}_{j_1} \bullet (-\vec{e}_{N,k} \times \vec{p}_k) + \vec{\omega}_{j_1} \bullet (\vec{e}_{N,k} \times \vec{p}_k) - \varepsilon_{\phi\phi} r_0 \sin\theta_{0k} \Delta\phi_1 - \varepsilon_{\phi\phi} r_0 \Delta\theta_1 + \varepsilon_{\phi\theta} r_0 \sin\theta_{0k} \Delta\phi_2 + \varepsilon_{\theta\theta} r_0 \Delta\theta_2$$
$$= \left(a_k \delta\vec{G}_{SS,k} + b_k \delta\vec{G}_{N,k}\right) \bullet \vec{e}_N$$

$$\vec{\omega}_{j_1} \bullet (-\vec{e}_{E,k} \times \vec{p}_k) + \vec{\omega}_{j_1} \bullet (\vec{e}_{E,k} \times \vec{p}_k) - \varepsilon_{\phi\phi} r_0 \sin\theta_{0k} \Delta\phi_1 - \varepsilon_{\phi\theta} r_0 \Delta\theta_1 + \varepsilon_{\phi\theta} r_0 \sin\theta_{0k} \Delta\phi_2 + \varepsilon_{\theta\theta} r_0 \Delta\theta_2$$
$$= \left(a_k \delta\vec{G}_{SS,k} + b_k \delta\vec{G}_{N,k}\right) \bullet \vec{e}_E$$

Acknowledgments

We would like to thank the National Science Foundation (projects EAR-0610031 and EAR-0635757) and Department of Energy for support of various aspects of this project including data collection, processing, modeling and interpretation. The Department of Energy support comes from a grant through the Great Basin Center for Geothermal Energy at the University of Nevada, Reno and from the Yucca Mountain Task 3, "Geodetic Monitoring of the Yucca Mountain Region using Continuous Global Positioning System Measurements" Our block modeling in the western Great Basin is also supported by the National Earthquake Hazards Reduction Program (Announcement 07HQPAQ0001 - Proposal 2007-0040).

References

Bennett, R. A., W. Rodi, and R. E. Reilinger (1996), Global Positioning System constraints on fault slip rates in southern California and northern Baja, Mexico, J. Geophys. Res., 101(B10), 21,943 - 21,960.

England, P., and D. McKenzie (1982), A thin viscous sheet model for continental deformation, Geophys. J. Roy. Astron. Soc., 70, 295-321.

Gourmelen, N., and F. Amelung (2005), Post-seismic deformation in the central Nevada seismic belt detected by InSAR: Implications for Basin and Range dynamics, Science, 310, 1473-1476.

Hammond, W. C., C. Kreemer, and G. Blewitt (2007), Geodetic constraints on contemporary deformation in the northern Walker Lane: 3, Postseismic relaxation in the Central Nevada Seismic Belt, Late Cenozoic Structure and Evolution of the Great Basin – Sierra Nevada Transition, J.Oldow and P.Cashman eds, in review.

Hammond, W. C., and W. Thatcher (2007), Crustal Deformation across the Sierra Nevada, Northern Walker Lane, Basin and Range Transition, western United States Measured with GPS, 2000-2004, J. Geophys. Res., in press.

Kreemer, C., G. Blewitt, and W. C. Hammond (2007), Geodetic constraints on contemporary deformation in the northern Walker Lane: 2, velocity and tensor strain rate analysis, Late Cenozoic Structure and Evolution of the Great Basin – Sierra Nevada Transition, J.Oldow and P.Cashman eds, in review.

McCaffrey, R. (Ed.) (2002), Crustal block rotations and plate coupling, 101-122 pp., AGU Geodynamics Series, v30.

McCaffrey, R. (2005), Block kinematics of the Pacific-North America plate boundary in the southwestern United States from inversion of GPS, seismological and geologic data, J. Geophys. Res., 110, B7, doi:10.1029/2004JB002207.

McClusky, S. C., S. C. Bjornstad, B. H. Hagar, R. W. King, B. J. Meade, M. Miller, F. C. Monastero, and B. J. Souter (2001), Present Day kinematics of the Eastern California Shear zone from a geodetically constrained block model, Geophys. Res. Lett., 28(17), 3369-3372.

Meade, B. J., and B. H. Hagar (2005), Block models of crustal motion in southern California constrained by GPS measurements, J. Geophys. Res., 110, B03403, doi:10.1029/2004JB003209.

Murray, M. H., and P. Segall (2001), Modeling broad scale deformation in northern California and Nevada from plate motions and elastic strain accumulation, Geophys. Res. Lett., 28, 4315-4318.

Okada, Y. (1985), Surface deformation due to shear and tensile faults in a half-space, Bull. Seismol. Soc. Am., 75(4), 1135-1154.

Okada, Y. (1992), Internal deformation due to shear and tensile faults in a half-space, Bull. Seismol. Soc. Am., 82(2), 1018-1040.

Prawirodirdjo, L., Y. Bock, R. McCaffrey, J. F. Genrich, E. Calais, C. Stevens, S. S. O. Puntodewo, C. Subarya, J. Rais, P. C. Zwick, and Fauzi (1997), Geodetic observations of interseismic strain segmentation at the Sumatra subduction zone, Geophys. Res. Lett., 24, 2601-2604.

Savage, J. C. (1983), A dislocation model of strain accumulation and release at a subduction zone, J. Geophys. Res., 88(6), 4984-4996.

Savage, J. C., and R. O. Burford (1973), Geodetic determination of relative plate motion in central California, J. Geophys. Res., 78(85), 832-845.

Savage, J. C., W. Gan, and J. L. Svarc (2001), Strain accumulation and rotation in the eastern California shear zone, J. Geophys. Res., 106(B10), 21,995-922,007.

Souter, B. J. (1998), Comparisons of geological models to GPS observations in southern California, Ph.D. thesis, Cambridge, MA.

Thatcher, W. (1995), Continuum versus microplate models of active continental deformation, J. Geophys. Res., 100, 3885-3894.

Thatcher, W. (2003), GPS constraints on the kinematics of continental deformation, Internat. Geol. Rev., 45, 191-212.

Wesnousky, S. G. (2005), Active faulting in the Walker Lane, Tectonics, 24(TC3009, doi:10.1029/2004TC001645)